International Journal of Engineering Research & Technology (IJERT)
ISSN: 2278-0181
Vol. 14, Issue 08, IESAME - 2026

Microstructural Variations in FSW Al6061-Al7075: A Comparative SEM Study Based on Tensile Performance

Mahendra K C[1]
Assistant Professor,
Rao Bahadur Y. Mahabaleswarappa Engineering College
Ballari, Karnataka, India
Mahendra.kc@rymec.in

Virupaksha Gouda H[2]
Assistant Professor
Rao Bahadur Y. Mahabaleswarappa Engineering College
Ballari, Karnataka, India
Virupaksha.gouda@rymec.in

Channaveera Swamy J M[3]
Assistant Professor
Rao Bahadur Y. Mahabaleswarappa Engineering College
Ballari, Karnataka, India
cv.swamy@rymec.edu.in

Manjunath M H[4]
M.Tech Student,(MPM)
Rao Bahadur Y. Mahabaleswarappa Engineering College
Ballari, Karnataka, India
Manjunathmh671@gmail.com

***Abstract*— Friction stir welding (FSW) of dissimilar Al6061 and Al7075 alloys offers a reliable solid-state joining method, yet microstructural inconsistencies often dictate overall joint integrity. This study investigates the direct correlation between weld microstructure and mechanical performance. A total of 31 FSW specimens were fabricated and evaluated for tensile strength. Based on these baseline results, six targeted samples representing high, medium, and low tensile performance (two of each) were isolated for detailed Scanning Electron Microscopy (SEM) characterization. By comparing these specific performance tiers, this research identifies the precise microstructural defects, material flow patterns, and grain formations that govern tensile failure in dissimilar aluminum welds.**

Keywords: Aluminum alloys; friction stir welding; Scanning Electron Microscopy (SEM).

I. INTRODUCTION

The demand for lightweight, high-strength materials in the automotive and aerospace sectors has driven extensive research into aluminum alloys, particularly Al6061 and Al7075. While these alloys offer exceptional strength-to-weight ratios, joining them via conventional fusion welding presents significant engineering challenges, including severe hot cracking, porosity, and a drastic reduction of mechanical properties in the fusion zone. Friction Stir Welding (FSW), a solid-state joining technique, has emerged as a highly effective solution. By utilizing a non-consumable rotating tool to generate frictional heat and plastically deform the material, FSW facilitates the bonding of dissimilar aluminum alloys without reaching their melting points. However, the resulting weldment is highly complex, comprising distinct microstructural regions such as the stir zone (SZ), thermo-mechanically affected zone (TMAZ), and heat-affected zone (HAZ). The dynamic material flow and thermal cycles experienced during the FSW process directly dictate the formation of these zones, which ultimately govern the overall mechanical integrity and load-bearing capacity of the joint.

II. LITERATURE SURVAY

P. Wawrzyniak, R. Kosturek, J. Torzewski, D. Klápště, and J. Moravec S. (Manufacturing of Dissimilar 6061–7075 Aluminum Alloy Joints Via Friction Stir Welding) in This study investigates the microstructural integrity and tensile behavior of joining high-strength Al7075 with Al6061 via FSW. The researchers demonstrate how shifting the tool offset alters material mixing in the stir zone, utilizing microscopy and tensile testing to map grain boundary formations against actual mechanical failure points.

M. A. Al-Kinani et.al. (Optimizing Tensile Strength and Hardness in FSW of AA 6061 and AA 7075 via RSM and Desirability Function) Employing Response Surface Methodology (RSM), this research systematically correlates primary FSW operational parameters—specifically tool rotational speed and linear welding feed—to the final mechanical properties of the joint. Scanning electron microscopy (SEM) is heavily featured to analyze the fracture surfaces, linking internal microstructural anomalies directly to variations in ultimate tensile strength.

M. Safari, R. A. de Sousa, J. Joudaki, and H. Mostaan (Experimental Investigation of Weld Quality for Dissimilar Welding of AA6061-T6/AA7075-T6 Aluminum Alloys) This paper offers an experimental breakdown comparing the tensile strength and microstructural evolution of FSW Al6061/Al7075 joints against traditional fusion methods. The authors closely examine how dynamic recrystallization and material flow govern the size of equiaxed grains in the melt zone, directly influencing the joint's overall load-bearing capacity.

International Journal of Engineering Research & Technology (IJERT)
ISSN: 2278-0181
Vol. 14, Issue 08, IESAME - 2026

G. Bharath, G. Kishor Kumar, and R. Sagar (Optimization of Process Parameters for Al6061-Al7075 Alloys in Friction Stir Welding Using Taguchi's Technique) Utilizing a robust Taguchi experimental design array, this study isolates the optimal combination of rotational speed, welding speed, and tool tilt angle for dissimilar aluminum FSW. The research focuses on maximizing ultimate tensile strength (UTS) and hardness, detailing the underlying microstructural conditions that allow for high-strength, defect-free metallurgical bonding.

III.PROBLEM STATEMENT

Despite the proven viability of FSW for joining dissimilar Al6061 and Al7075 plates, a critical gap remains in understanding the precise microstructural mechanisms that dictate varying levels of tensile performance within the same operational framework. Much of the existing literature evaluates average joint efficiencies or focuses broadly on parameter optimization, without directly comparing the internal anomalies that cause premature failure against the structural characteristics that yield optimal strength. When welding dissimilar alloys, uneven material mixing, variations in precipitate distribution, and micro-void formation can lead to significant inconsistencies in joint reliability. There is a pressing need to systematically isolate and analyze the microstructural differences between high-performing and underperforming welds. This study addresses this gap by conducting a targeted comparative analysis. By correlating distinct tiers of tensile performance with their corresponding Scanning Electron Microscope (SEM) data, this research aims to identify the specific micro-level factors such as grain structure and defect distribution that govern macro-level tensile failure in FSW Al6061-Al7075 joints.

IV.METHODOLOGY

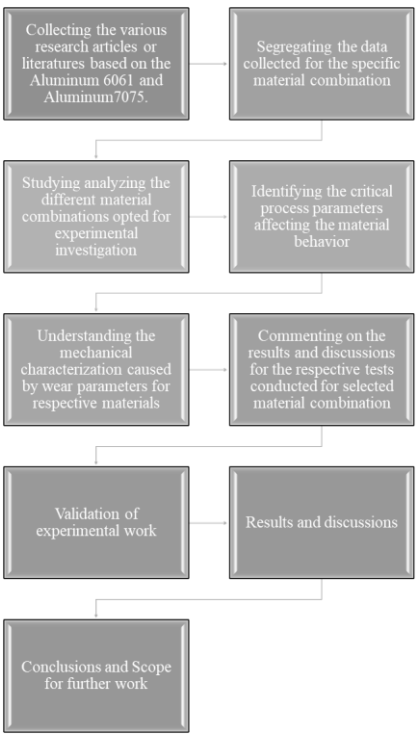

V. EXPERIMENTAL DETAILS

1) Material selection

Based on the literature review and feasibility of research topic present investigation considered Al 6061 & Al 7075 of 6 mm thickness as the base metal. The material properties of these alloys include good fatigue strength, machinability and less resistance to corrosion than other aluminium alloys. chemical, physical and mechanical properties were stated in the following table1, & table 2 respectively

Table 1 Chemical composition of AA7075 T6 and AA6061 T6

Constituents	AA6061 T6	AA7075 T6
Aluminium	90.311	97.766
Chromium	0.2	0.064
Copper	1.31	0.19
Iron	0.17	0.25
Magnesium	2.28	0.8
Manganese	0.019	0.12
Zinc	5.61	0.11
Silicon	0.1	0.7

Table 2 Physical properties of AA7075 T6 and AA6061T6

Material	AA 6061 T6	AA 7075 T6
Density (kg/m3	2700	2800
Melting Point (0C)	650	477
Modulus of elasticity (GPa)	70	71.7
Thermal Conductivity (w/MK)	166	130-150

In the present study, receive draw material dimensions were different at the initial state condition as shown fig 3. To suit the requirements needed, the rolled plates of aluminium alloys were remodified with proportions of140 x 70 x 6 mm with the help of CNC machine. To facilitate the insertion of nanoparticles in the workpiece abutting edges, separate holes of depth 4mm and 10 mm apart from subsequent holes were drilled at the peripheral state of both the alloys as shown below.

Figure 1 Base plates of Al6061 and Al7075 were machined to specified dimensions

2) Preparation of Specimen

To execute this comparative study, base plates of Al6061 and Al7075 were machined to specified dimensions and securely clamped in a square butt joint configuration as shown in the figure 2. The FSW process was carried out using a designated rotating tool, ensuring solid-state bonding across the dissimilar interface. Following the welding phase, a total of 31 transverse tensile specimens were extracted perpendicular to the weld

International Journal of Engineering Research & Technology (IJERT)
ISSN: 2278-0181
Vol. 14, Issue 08, IESAME - 2026

direction in accordance with standard ASTM testing guidelines. All 31 specimens were subjected to tensile testing to failure to establish a comprehensive mechanical performance baseline. From these results, six specific specimens were strategically isolated for advanced microstructural evaluation: two representing the highest tensile strength, two representing the median (medium) performance, and two exhibiting the lowest tensile strength. These six selected samples were sectioned at the weld zone, mounted, and subjected to rigorous metallographic preparation. This process involved sequential grinding with graded silicon carbide emery papers, followed by fine polishing with diamond paste to achieve a mirror-like finish. Finally, the specimens were etched using Keller's reagent to reveal grain boundaries and distinct material flow patterns prior to detailed SEM characterization.

Figure 2 Frictions Stir Welding Fixture Setup and Welding Tool

3) Tensile Test

To evaluate the mechanical integrity of the dissimilar FSW Al6061-Al7075 joints, tensile testing is executed in strict accordance with the ASTM E8/E8M standard. Initially, the welded plates are machined into transverse dog-bone specimens as shown in the figure 3, ensuring that the entire weldment including the stir zone, thermo-mechanically affected zone (TMAZ), and heat-affected zone (HAZ) is centrally isolated within the gauge length. After meticulously recording the initial cross-sectional dimensions using a digital micrometer, each specimen is vertically aligned and secured into the wedge grips of a Universal Testing Machine (UTM), shown in the figure 4, with an extensometer affixed to precisely monitor localized strain. A continuously increasing uniaxial load is applied at a controlled, constant extension rate until complete macroscopic rupture occurs, which frequently localizes in the structurally softer heat-affected zone of the Al6061 side. The testing apparatus simultaneously records the load and displacement metrics to generate a continuous stress-strain curve, allowing for the precise extraction of ultimate tensile strength (UTS), yield stress, and percentage elongation to accurately rank the 31 specimens for the subsequent targeted SEM evaluation.

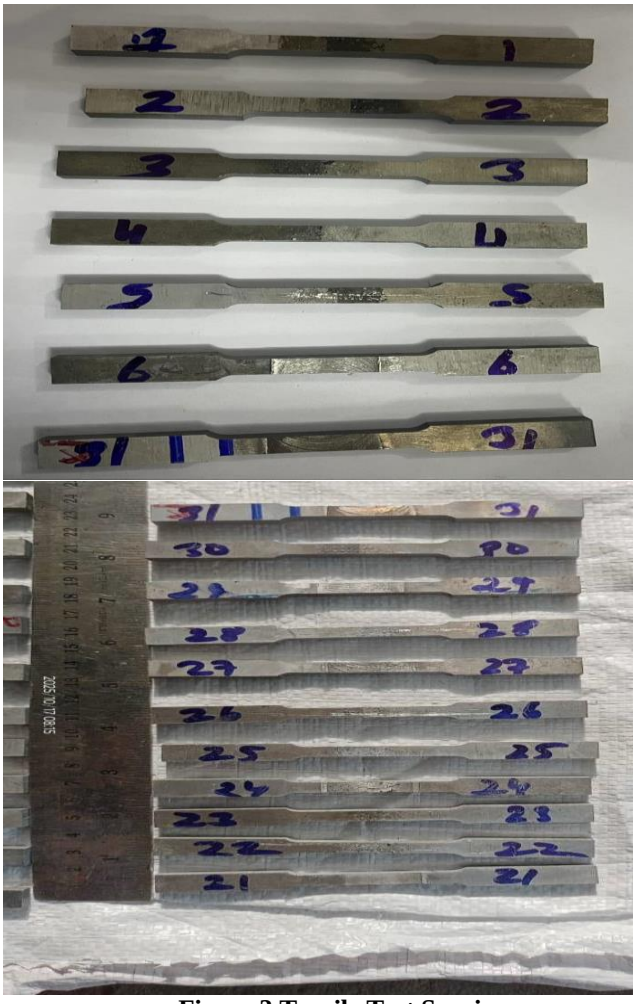

Figure 3 Tensile Test Specimens

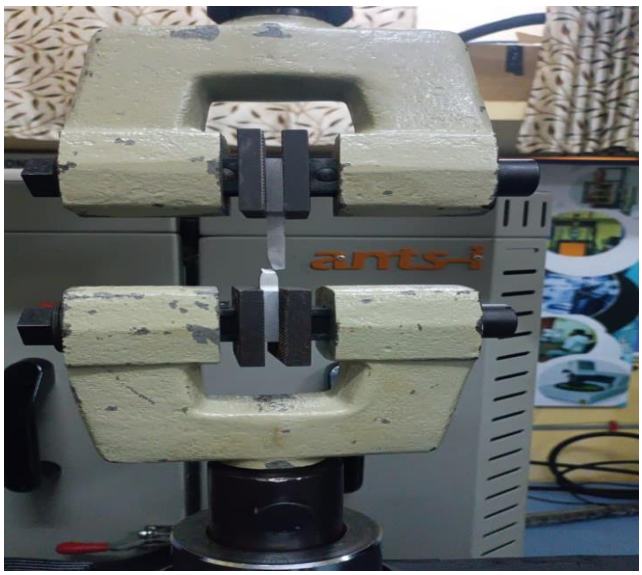

Figure 4 Universal Testing Machine (UTM)

International Journal of Engineering Research & Technology (IJERT)
ISSN: 2278-0181
Vol. 14, Issue 08, IESAME - 2026

Table 3 Tensile Strength Results

Sl no	Sample Details	Tensile Strength (Mpa)	Criteria
1	Sample -8	78	Low Tensile Strength
2	Sample -9	81	Low Tensile Strength
3	Sample -11	96	Mid Tensile Strength
4	Sample -17	99	MidTensile Strength
5	Sample -18	144	High Tensile Strength
6	Sample -20	139	High Tensile Strength

From experimental tensile tests 31 specimens were tested. Based on the strength obtained, two high, Mid & low Specimens were selected for further observations

4) Scanning Electron Microscope (SEM)

Following the tensile evaluation, the six isolated specimens representing the two highest, two median, and two lowest performing joints undergo detailed microstructural and fractographic analysis using a Scanning Electron Microscope (SEM). In the laboratory, preparation begins by precision-cutting the fractured interfaces and the transverse weld zones into small sections that can easily fit inside the SEM vacuum chamber. To ensure clear imaging and prevent electrical charging artifacts under the electron beam, these metallic samples are securely mounted onto aluminum stubs using highly conductive double-sided carbon tape. For the evaluation of internal grain structures, the cross-sections are typically embedded in epoxy resin, polished to a mirror-like finish using diamond suspensions, and lightly etched with Keller's reagent to reveal the distinct flow patterns between the Al6061 and Al7075 alloys. Once prepared, the specimens are placed inside the high-vacuum chamber. The SEM directs a focused, high-energy electron beam across the sample, capturing the emitted secondary and backscattered electrons to construct high-resolution topographical images. For these six specific FSW joints, this process directly visually compares the fracture surfaces identifying ductile dimples, brittle cleavage planes, micro-voids, or incomplete mixing to precisely explain why each specimen achieved its specific high, medium, or low tensile ranking.

VI.RESULTS AND DISCUSSION

1) Tensile Test

The transverse tensile testing of the friction stir welded Al6061-Al7075 joints revealed a wide spectrum of mechanical load-bearing capabilities, driven by the varying process parameters across the 31 original specimens. To systematically understand this variation, the data was stratified into three distinct performance tiers based on the Ultimate Tensile Strength (UTS) recorded at the point of fracture. The transverse tensile testing of the friction stir welded Al6061-Al7075 joints revealed a wide spectrum of mechanical load-bearing capabilities, driven by the varying process parameters across the 31 original specimens. To systematically understand this variation, the data was stratified into three distinct performance tiers based on the Ultimate Tensile Strength (UTS) recorded at the point of fracture.

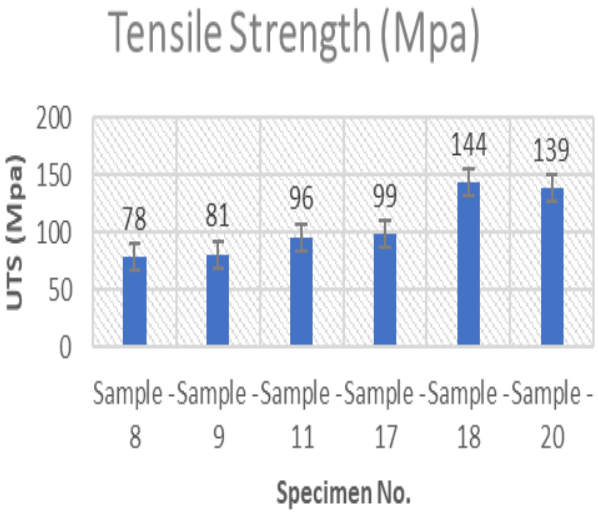

Figure 5 Tensile Test Results

The transverse tensile testing of the friction stir welded Al6061-Al7075 joints revealed a wide spectrum of mechanical load-bearing capabilities, driven by the varying process parameters across the 31 original specimens. To systematically understand this variation, the data was stratified into three distinct performance tiers based on the Ultimate Tensile Strength (UTS) recorded at the point of fracture.

Low Tensile Performance (Samples 8 and 9):
The lowest performing joints in the study, Sample 8 and Sample 9, yielded ultimate tensile strengths of only 78 MPa and 81 MPa, respectively. These severely depressed values indicate a fundamental failure to establish a continuous metallurgical bond between the dissimilar alloys. A tensile strength in this lower threshold strongly suggests that the specific FSW parameters used for these welds generated insufficient frictional heat or inadequate plunging force. Consequently, the material failed to plasticize properly, leading to a weak interface that easily ruptured under minimal axial loading.

Median Tensile Performance (Samples 11 and 17):
Samples 11 and 17 demonstrated a moderate, transitional mechanical capacity, recording UTS values of 96 MPa and 99 MPa. This represents an approximate 22% increase in strength compared to the lowest tier, proving that the material mixing and thermal input were significantly improved. However, the plateau just below the 100 MPa mark implies that while a contiguous joint was successfully formed, localized structural weaknesses remained. This median performance is typically the result of thermal softening in the Heat-Affected Zone (HAZ) or the presence of minor, sub-surface intermixing flaws that act as stress concentrators, ultimately preventing the joint from reaching its maximum potential strength.

High Tensile Performance (Samples 20 and 18)
The peak mechanical integrity of the experimental batch was observed in Sample 20 and Sample 18, which achieved impressive UTS values of 139 MPa and 144 MPa. Representing an 84% strength increase over Sample 8, these

International Journal of Engineering Research & Technology (IJERT)
ISSN: 2278-0181
Vol. 14, Issue 08, IESAME - 2026

results confirm the execution of an optimal FSW parameter combination. The ability to withstand stresses exceeding 140 MPa signifies an excellent thermodynamic balance during the welding process. At these parameters, the Al6061 and Al7075 base metals achieved thorough plastic flow and dynamic recrystallization in the stir zone. This produced a highly consolidated, defect-free joint capable of superior load transfer, thereby maximizing the overall joint efficiency before eventual failure

2) SEM Analysis

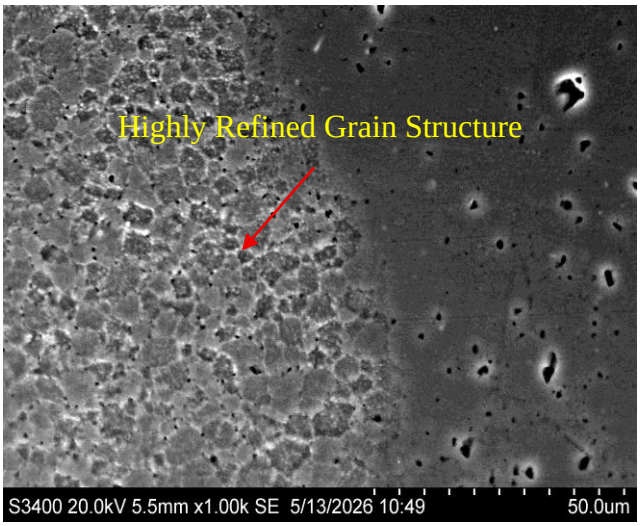

Figure 6 High Tensile Specimen 01

Scanning Electron Microscope (SEM) micrographs reveal the microstructural characteristics of the material's failure zones, establishing a direct correlation between grain structure, interfacial boundaries, and the previously recorded tensile strength values. In the low tensile strength specimens, the higher-magnification images reveal a coarse, distinctly outlined grain structure interspersed with a high concentration of microvoids and precipitates segregated along the grain boundariesas shown in Figure 01 and 02. When subjected to tensile loading, these boundary defects act as severe stress concentrators, promoting rapid void coalescence. This induces a classic intergranular fracture pathway, as evidenced by the wide, continuous, and relatively straight crack propagation visible in the lower-magnification images. Because the crack encounters minimal structural resistance along these weakened pathways, the material fails prematurely at lower stress levels 78-81 Mpa.

As processing modifications shift the material into the medium tensile strength category 96-99\ MPa, the microstructural landscape undergoes a visible refinement. The grain size appears more tightly controlled, and the interface line exhibits a slight increase in tortuosity compared to the low-strength samples.

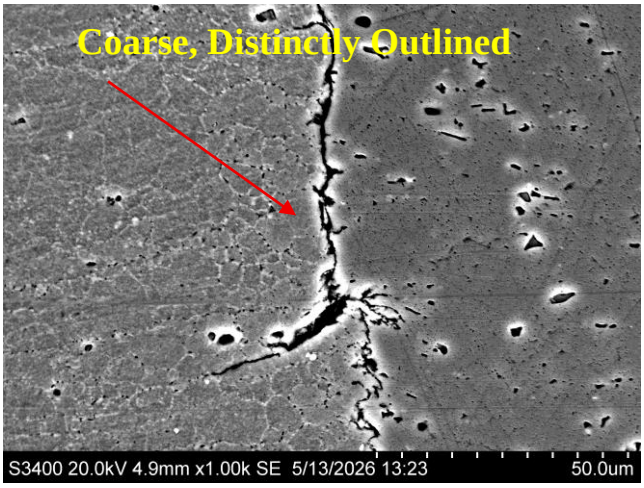

Figure 7 Low Tensile Specimen 01

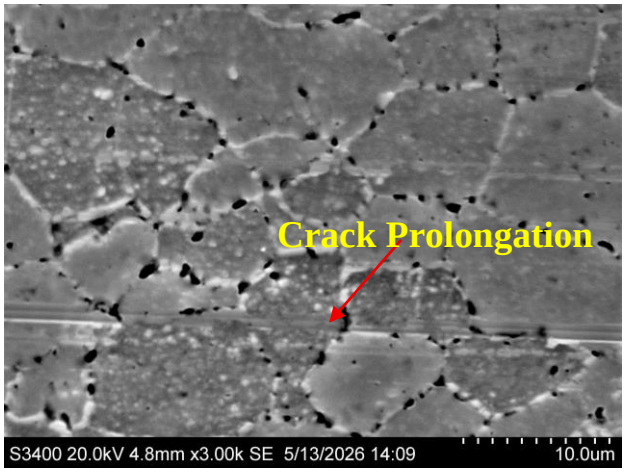

Figure 8 Low Tensile Specimen 02

As processing modifications shift the material into the medium tensile strength category 96-99\ MPa, the microstructural landscape undergoes a visible refinement. The grain size appears more tightly controlled, and the interface line exhibits a slight increase in tortuosity compared to the low-strength samples. This structural adjustment forces propagating cracks to deviate slightly from a straight path, absorbing more mechanical energy during deformation. While microvoids and secondary phase inclusions are still present, their distribution is marginally more dispersed, which delays the onset of critical microcrack linking. Consequently, the material can withstand greater plastic deformation and higher tensile loads before the propagation of a macroscopic crack triggers final structural failure.

The high tensile strength specimens 139-144 MPS demonstrate an entirely transformed microstructure characterized by an exceptionally fine, dense, and highly interlocked sub-grain network. At 1.00 Kx & 3.00 Kx times magnifications, the fracture or boundary line is remarkably jagged, convoluted, and non-linear.

International Journal of Engineering Research & Technology (IJERT)
ISSN: 2278-0181
Vol. 14, Issue 08, IESAME - 2026

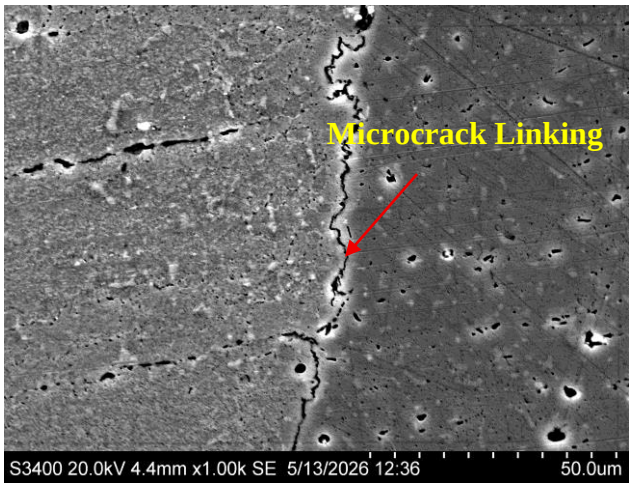

Figure 9 Mid Tensile Specimen 01

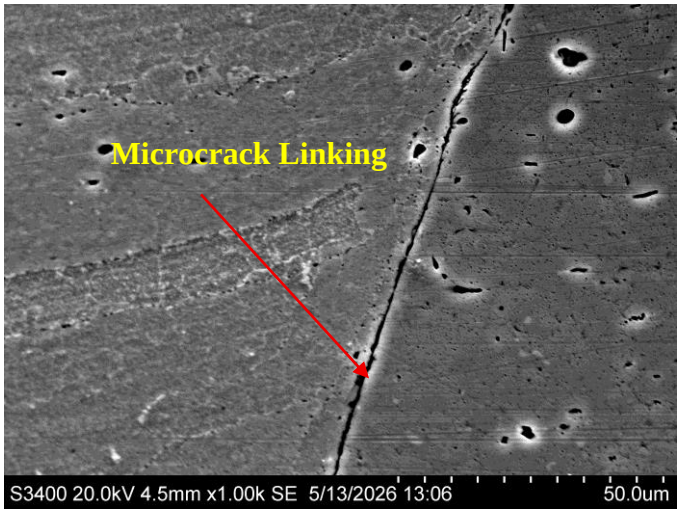

Figure 10 Mid Tensile Specimen 02

The high tensile strength specimens 139-144 MPS demonstrate an entirely transformed microstructure characterized by an exceptionally fine, dense, and highly interlocked sub-grain network. At 1.00 Kx & 3.00 Kx times magnifications, the fracture or boundary line is remarkably jagged, convoluted, and non-linear. This interlocking morphology severely hinders crack propagation through a mechanism known as crack deflection, where the crack path is forced to constantly change direction, dissipating massive amounts of strain energy. Furthermore, the highly refined grain structure dramatically increases the total grain boundary surface area, effectively distributing applied tensile stresses more uniformly and limiting the detrimental clustering of microvoids. This superior microstructural resistance directly accounts for the nearly doubled load-bearing capacity observed during the tensile test.

VII. DISCUSSIONS AND CONCLUSIONS

The investigation establishes a definitive structure-property relationship between the material's microstructural architecture and its macroscopic mechanical performance. The data reveals that tensile strength is inversely proportional to grain size and directly dependent on the tortuosity of internal boundaries. Low tensile strength samples (78-81 MPa) are limited by a coarse grain structure and a high density of grain-boundary microvoids, which facilitate rapid, low-energy intergranular fracture. Microstructural refinement in the medium-strength specimens (96-99MPa) provides a moderate barrier to crack propagation, resulting in improved load tolerance. Ultimately, the high tensile strength specimens (139-144 MPa) achieve peak mechanical performance due to a highly refined, dense sub-grain network and heavily interlocking interfaces. This specialized morphology forces severe crack deflection and dissipates substantial strain energy, effectively doubling the material's load-bearing capacity and validating the efficacy of the underlying processing optimizations.

VIII. REFERENCES

[1]. ASM Hand book, Selection and properties of non-ferrous materials, vol. 2. Ohio: ASM International, Metal Park; 1989. p. 1223–40.

[2]. Prasad BK. Engineering materials. Bombay: TMH; 1989. p. 20–50.

[3]. Dwivedi DK, Sharma Ashok, Rajan TV. Methods to improve the structure and properties of cast Al–Si alloys. Ind Foundry J 2000;46(12):31–9 [December].

[4]. ASM Handbook. Friction, wear and lubrication. Ohio: ASM International, Metal Park; 1989. p. 785–91.

[5]. Siva Ramakrishnan CS, Mahanti RK, Kumar R. Stir cast morphology of aluminum– silicon alloys. Aluminum 1981;57(12):820–1.

[6]. Avner SD. An introduction to physical metallurgy. London: Mc Graw Hill; 1999.

[7]. Dwivedi DK, Arjun TS, Thakur P, Vaidya H, Singh K. Sliding wear and friction behavior of Al–18%Si–0.5%Mg alloy. Mater Process Technol 2004;152(3):323–8.

[8]. R. Karthigeyan, G. Ranganath, S. Sankaranarayanan "Mechanical Properties and Microstructure Studies of Aluminum (7075) Alloy Matrix Composite Reinforced with Short Basalt Fiber" European Journal of Scientific Research, ISSN 1450-216X Vol.68 No.4 (2012), pp. 606- 615.

[9]. Arun Kumar D T, Raghavendra Rao P S, Mohammed Shadab Hussain, Naga Sai Balaji P R "Wear Behavior and Microstructure Analysis of Al-7075 alloy reinforced with Mica and Kaolinite" IOP Conf. Series: Materials Science and Engineering 376 (2018) 012067.

[10]. Madhuri Deshpande, Rahul Waikar, Ramesh Gondil, S.V. S Narayan Murty, T.S. Mahata "Processing of Carbon fiber reinforced Aluminum (7075) metal matrix composite" International Journal of Advanced Chemical Science and Applications (IJACSA), ISSN (Online): 2347-761X, Volume - 5, Issue -2, 2017.

[11]. Jamaluddin Hindi, Achuta Kini U, S.S Sharma "Mechanical Characterisation of Stir Cast Aluminum 7075

Matrix Reinforced it Grey Cast Iron & Fly Ash" International Journal
of Mechanical and Production Engineering, ISSN: 2320-2092. Volume- 4, Issue-6, Jun.- 2016.

[12]. Deepak Singla, S.R. Mediratta, "Evaluation of Mechanical Properties of Al 7075-fly Ash Composite Material", International Journal of Innovative Research in Science,
Engineering and Technology [IJIRSET], Vol 2, Issue 4, April 2013, pp 951 – 959

[13]. Niranjan K N, Shiva raj B N, Sunil Kumar M, Deepak A R, "Study of mechanical properties on AL 6061 hybrid composite by stir casting method", International research journal of engineering and technology [IRJET], Vol04, Issue 01, jan 2017, p-ISSN:2395- 0072

[14]. Madhuri Deshpande, Rahul Waikar, Ramesh Gondil, S.V. S Narayan Murty, T.S. Mahata "Processing of Carbon fiber reinforced Aluminum (7075) metal matrix composite" International Journal of Advanced Chemical Science and Applications (IJACSA), ISSN (Online): 2347-761X, Volume - 5, Issue -2, 2017.

[15]. Rabinowitcz E. Friction, wear and lubrication. New York: John Wiley and Sons; 1965. p. 70–118

[16]. G.B. Veeresh Kumar, C.S.P. Rao, N. Selvaraj, M.S. Bhagyashekar, "Studies on Al6061- Sic and Al7075- Al2O3 Metal Matrix Composites", Journal of Minerals and Materials Characterization and Engineering [JMMCE], Vol 9, Issue 1, 2010, pp 43 – 55.

[17]. Prashant S D, Sushil dange, "experimental analysis of aluminum alloys for aerospace application" IRJET, e-ISSN: 2395-0056, p-ISSN: 2395-0072 Vol: 06 issue:03 Mar 2019.

[18]. Arun Kumar D T, Raghavendra Rao P S, Mohammed Shadab Hussain, Naga Sai Balaji P R "Wear behavior and Microstructure Analysis of Al-7075 alloy reinforced with Mica and Kaolinite" IOP Conf. Series: Materials Science and Engineering 376 (2018) 012067.

[19]. American Society for Testing and Material, Annual Book of ASTM Standards. (USA, 1999)

[20]. K. Umanath, S.T. Selvamani, K. Palanikumar, Friction and wear behavior of Al6061 alloy (Sic? Al2O3P) hybrid composites. Int. J. Eng. Sci. Technol. 3(7), 5441–5451 (2011).